Integrated Head and Thorax Protection Evaluation for VRU Safety: A Simulation Based Approach

Dhaval Jani, Holger Staack, Christian Teichmann

Abstract Pedestrian injuries in road traffic collisions remain a significant global public health concern. While ongoing efforts by Original Equipment Manufacturers (OEMs), regulatory bodies, and consumer safety organizations have contributed to reduce the frequency and severity of pedestrian injuries, recent studies raised concerns if the vehicle design compliant to current safety protocols adequately addresses thoracic protection in vehicle–pedestrian impacts.

This study investigates whether headform impactor tests, as prescribed by the European New Car Assessment Programme Vulnerable Road User (VRU) Test Protocol, contributing to minimise head injury risk also furthers thoracic protection. A total of 974 headform impactor simulations were performed using both child and adult headforms. In parallel, 240 full-body vehicle–pedestrian impact simulations were conducted using detailed finite element (FE) models of the human body and production vehicles, accounting for various pedestrian, vehicle, and event-related parameters. The results indicated that the serious thoracic injuries (Abbreviated Injury Scale 3+ (AIS3+)) were exceedingly rare among the evaluated vehicle types. The majority of observed AIS2+ injuries were associated with the bonnet zones with higher Head Injury Criteria (HIC) values, while thoracic AIS2+ injuries in the bonnet regions with low HIC values were rare exceptions. Authors posit that the vehicle designs complying with existing pedestrian safety protocols may be complementing to reduce severity of thoracic injuries, potentially rendering additional thorax – specific tests superfluous.

Keywords Headform impactor, pedestrian safety, pedestrian thorax, thorax impactor.

I. INTRODUCTION

Road traffic deaths and injuries continue to pose a significant global health challenge. Among these, pedestrian injuries have emerged as a growing public health concern worldwide [1]. Each year, millions of pedestrians are injured, with many suffering life-altering disabilities. Alarmingly, an estimated 1.19 million lives were lost to road traffic incidents in 2021, with pedestrians accounting for 21% of fatalities [2]. In Europe alone (excluding Lithuania and Slovakia), 5,320 pedestrian deaths were reported in 2016, accounting for 21% of all road fatalities [3].

Vehicle-pedestrian collisions are complex events, where outcomes are influenced by numerous factors, including pedestrian attributes (e.g., age, gender, anthropometry, posture), vehicle characteristics (e.g., type, mass, structural stiffness, geometry), and impact parameters (e.g., speed, orientation, point of contact). Over the past decades, numerous studies have examined accident statistics and injury distributions, with particular emphasis on injury severity, especially concerning thoracic injuries in pedestrians. For the examined 80 pedestrian accidents in Australia, six cases with AIS2+ and 6 with AIS3+ thoracic injuries were found [4]. Analysis of data from Hospital Episode Statistics (HES) in United Kingdom consisting of around 80,116 cases between 1997 and 2007, shows that about 7% of pedestrians struck by cars, pickups, or vans sustained thoracic injuries [5]. Data from the Rhône Trauma Registry in France indicated that among 3,289 cases, 281 (8.5%) involved AIS2+ thorax injuries, with around 70% of them affecting the rib cage [6]. In [7], data from the Swedish Traffic Accident Data Acquisition (STRADA) registry (2003–2017) were grouped by region, with thoracic injuries classified together with abdominal, spinal, and extremity injuries. This aggregation limits the ability to isolate thoracic injury data for detailed analysis. In the Vehicle Occupant Infrastructure Road User Safety Study (VOIESUR) database, it was observed that 7–8% of pedestrians sustained AIS2+ thoracic injuries, considerably lower in number compared to injuries to the head and limbs [3]. A similar trend was observed in the German In-Depth Accident Study (GIDAS) database [8]. Based on GIDAS data up to June 2021, it was reported that 13.6% of pedestrians suffered AIS2+ thoracic injuries across all

Dr. Dhaval Jani (Tel: +49 152 577 68383; e-mail: dhaval-ashvinkumar.jani@vaiva.io) is an Engineers at VAIVA GmbH in Gaimersheim, Germany. Dr.-Ing. Holger Staack and Christian Teichmann are Engineers at AUDI AG in Ingolstadt, Germany.

speeds, while 7.4% sustained thoracic injuries at speeds below 45 km/h [9]. In a follow-up study, it was reported that 7.8% of pedestrians in GIDAS suffered AIS2+ thorax injuries at low speeds, whereas in the China In-Depth Accident Study (CIDAS) database, this number was notably higher at 23% [10]. Further analysis revealed that the vehicle velocity [9-10], vehicle fronts like Van [9] and particularly pedestrian's age [10] were the parameters influencing the severity of the thoracic injuries. Across most datasets, thoracic injuries consistently rank third or fourth in terms of injury frequency, AIS3+ injuries to the thorax account for 7-8% of total thoracic injuries, and thoracic injuries tend to be a secondary consequence and rarely a single injury [9-10].

Analysis of the CIDAS database shows that that the most frequently occurring thoracic injuries are rib fractures accounting for approximately 59% of thoracic injuries involved. The study also highlighted that the relative height of the pedestrian's chest to the vehicle bonnet significantly influences thoracic injury severity [11].

Reducing the frequency and severity of pedestrian injuries is a complex, interdisciplinary task and requires a systematic approach involving engineering design improvements, law enforcement, and public awareness initiatives [12]. OEMs, legislators, and consumer safety organisations continue to collaborate towards making vehicles safer for pedestrians. Despite regional disparities, a global 5% reduction in pedestrian fatalities has been observed since 2010 [2]. The markets where the pedestrian protection enforcements are emphasised, have seen greater reductions in the pedestrian fatalities. For instance, pedestrian fatalities in Europe decreased by 38% between 2011 and 2023 [13]. Historically, efforts by OEMs and rating agencies have concentrated primarily on reducing head and lower extremity injuries [14]. However, recent studies evaluated thoracic injury risks as well [14-16]. To understand the mechanism and parameters influencing injury to the pedestrian thorax, various vehicle, and pedestrian configurations were analysed across different studies [14, 16-18]. Previous studies have highlighted the influence of factors, such as vehicle front geometry, impact speed, pedestrian anthropometry, impact location [16-17], as well as pedestrian posture and orientation [18], on pedestrian kinematics and the resulting injury outcomes. A correlation between the Head Injury Criterion (HIC) and rib deflection was demonstrated by [19], suggesting that reducing HIC may also help lower rib fractures. Few studies have investigated whether existing impactor tests can reliably reflect or correlate with thoracic protection performance. For instance, the relationship between rib deformation and head accelerations in lateral impacts was examined through simulations involving three vehicle types and three sizes of the Total Human Model for Safety (THUMS) v1.4 AM50 Human Body Models (HBMs) [20]. The findings, supported by simulated headform impacts at specific vehicle locations, indicate that headform tests following Japan New Car Assessment Program (JNCAP) protocols may also provide insights into chest protection, especially in cases involving vehicles with one-box designs and smaller pedestrians [20]. From the approach in [20], one can deduce that average acceleration measured in headform tests can serve as a proxy for local structural stiffness. Since thoracic injury risk in pedestrian impacts is also influenced by the stiffness of the contact area, particularly where the thorax strikes the bonnet, there is a biomechanical basis for the observed correlation between headform test results and thoracic injury outcomes. The influence of chest-to-bonnet height ratios on thoracic injury outcomes was examined by [11] and reported that legform impactor tests may partially reflect thoracic protection.

In the domain of VRU safety, headform impactor tests, mandated by both regulations and consumer rating bodies, have long played a central role in reducing head injuries. These tests typically assess injury risks over bonnet and windshield areas using HIC values. While head injury mitigation has traditionally been the primary focus of pedestrian safety design, it is worth exploring whether bonnet structures optimized to reduce head injuries also contribute to lowering the likelihood and severity of thoracic injuries. Since injury risk outcomes are highly dependent on both the affected body regions of pedestrian and vehicle contact location, efforts to minimize injuries to different body regions in a single vehicle area may result in design trade-offs. Therefore, this study aims to evaluate whether vehicle designs that meet pedestrian head protection requirements, assessed through headform impactor simulations as per Euro NCAP protocols [21], also inherently offer sufficient protection to the thorax, particularly in terms of reducing rib fractures.

II. METHODS

The methodology employed in this study follows the approach outlined in the authors' previous work [14] and is reproduced here for completeness. Detailed finite element (FE) models of three modern vehicles, sourced from the Volkswagen Group's vehicle fleet, were used in the study. The vehicle models were internally validated for various impact scenarios and legislative test cases. Two vehicles were sport utility vehicles (one midsize and another compact-midsize), and one was a sedan. The choice of the vehicles was governed by the fact that there is shift in the vehicle registration trend in Germany showing that 40% of the registered vehicle in 2024 were SUV and Off-Road vehicles (inferred from [22-23]). The sedan and one SUV were equipped with deployable bonnets, a safety feature intended to enhance the pedestrian head protection. To capture the effect of bonnet deployment, simulations were conducted with both deployed and undeployed configurations, resulting in five distinct vehicle variants. Two sets of simulations were performed: (1) Headform impactor simulations (adult and child) in accordance with [21], (2) Full-body vehicle-pedestrian impact simulations using the HBM.

Headform Impactor Simulations

This study utilized validated FE models of both adult and child headform impactors, developed in accordance with the Euro NCAP VRU test protocols [21]. These models were designed to accurately replicate the physical specifications outlined in the protocol, including mass, diameter, moment of inertia, and instrumentation layout outlined in UN-ECE R127 Revision 2 [24]. Their validity was confirmed through correlation with the experimental drop test response curves, as illustrated in Fig. A1. To ensure alignment with Euro NCAP guidelines and to capture a broad spectrum of potential HBM thorax contact areas, a headform impactor test grid (Fig. 1), defined in the Euro NCAP VRU Test Protocol [21], was employed.

Using the predefined grid point mapping for each vehicle model, headform impact locations were determined based on the Wrap Around Distance (WAD), a measurement that follows the vertical contour from the ground to various points on the vehicle's front surface. Depending on the WAD zone associated with each grid point, either an adult or child headform impactor was selected for the corresponding simulation.

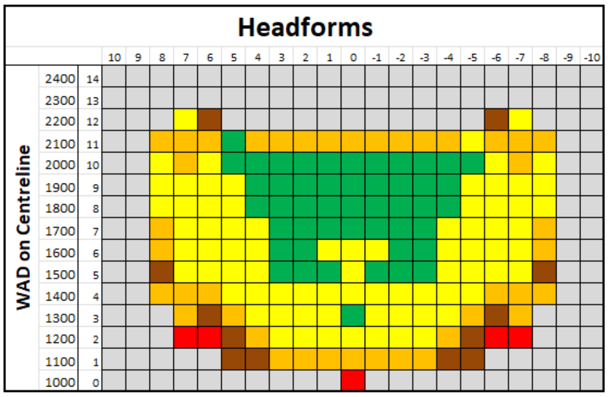

Fig. 1. Representative Headform Impactor Simulation Grid [21]

A total of 974 headform impact simulations were conducted across three vehicle models: two sedans (2 × 182 impacts), two SUV1 models (2 × 186 impacts), and one SUV2 model (238 impacts), covering the entire test area specified in the Euro NCAP protocol. In each headform impact simulation, the headform was launched at a speed of 40 km/h toward the bonnet, and the Head Injury Criterion over an interval of 15 milliseconds (HIC15) was calculated. To account for variability in thorax-to-vehicle contact which is strongly influenced by impact location, pedestrian posture, orientation, and vehicle type (representative positions in Fig. A2), a comprehensive series of headform impact simulations was conducted at predefined locations specified by the Euro NCAP VRU Protocol. By precomputing Head Injury Criterion (HIC) values at a wide range of grid points, aligned with Euro NCAP guidelines, it was possible to directly map the thorax contact region from any HBM scenario to the corresponding headform HIC data. This approach ensured consistent and protocol-compliant evaluation across all configurations.

HBM and Thoracic Injury Risk Prediction

The HBM used was based on the 50th percentile male THUMS v4.1 occupant model (VPS, ESI Group) positioned to required pedestrian posture(s), with further enhancements incorporated in lower extremities, pelvis, thorax and soft tissues [25-26], and head [27] to improve biofidelity of the model. After enhancing the model, the model was validated at various levels as shown in [25-27]. Additionally, the model response was also evaluated against full body tests described [28-29]. Good agreement was observed between simulation kinematics and experimental results. Full details of this validation are outside the scope of this manuscript. Following these validations, the model was certified according to the guidelines of EuroNCAP Technical Bulletin 024 (Version 4.0, dated July 23, 2023, now known as EuroNCAP Pedestrian Human Model Certification) [30], enabling its subsequent use for evaluation.

Injury risk functions for individual ribs were developed. The injury prediction function for a cumulative ribcage injury was developed using a methodology similar to [31], based on experimental datasets. The details of the development and validation of the maximum principal strain (MPS) based injury risk function (of the form of Eq. 1) used in the present study are available in [26].

$$P_{fracture} = 1 - e^{-\left(\frac{MPS}{scale\ factor}\right)^{shape\ factor}} \quad (1)$$

where $P_{fracture}$ is probability of fracture.

Validation of the injury risk function was performed using 23 real-world VRU and occupant cases, as part of AUDI AG's internal accident research. Using a 50% injury probability threshold, the injury/no-injury prediction of the model was found to be correct in 22 out of 23 cases [14].

HBM Simulations

In the HBM simulations, various parameters were systematically varied to address different attributes of vehicle - pedestrian accidents:

1. Leg Posture: The primary configuration was *Left Leg Forward (LLF)*, based on Euro NCAP TB024 guidelines (Fig. 2a). A mirrored version, *Left Leg Backward (LLB)*, was also used (Fig. 2b). Variations in leg posture not only influence the initial point of contact during impact but also significantly affect the pedestrian's post-impact kinematics, particularly rotation about Z-axis, thereby altering the nature and location of thoracic interaction with the vehicle.
2. Orientation: Pedestrian orientations of 60°, 90°, and 120° relative to the vehicle were considered (Fig. 3). The pedestrian's pre-impact orientation may influence post-impact rotational dynamics and wrap-around behavior, thereby contributing to variations in thoracic interaction with the vehicle.
3. Y-Location: Four lateral impact positions along the Y-axis were evaluated (center (Y000), 400 mm (Y400), 700 mm (Y700), and 800 mm (Y800) from the bumper center) (see Fig. 4). These positions were defined relative to the center of gravity (CoG) of the HBM's head. Variations in Y-impact locations help capture the influence of differing bonnet geometries, which in turn lead to variations in post-impact thoracic loading.
4. Upper Extremity Interaction: For each configuration, two simulation variants were conducted, one allowing contact between the upper extremities and the vehicle (*WCNT*), and one without the contact (*WoCNT*). Shoulder contact was enabled in both cases. At the time of impact, a pedestrian's upper extremities can adopt various postures (Fig. A2), which significantly influence how the upper extremities interact with the vehicle and loading of the thorax due to the interaction of the upper extremities with the vehicle. The interaction of the thorax with the vehicle plays a key role in rib deflection and, consequently, in the severity of the injuries sustained. As also reported in [16], upper extremity positioning generally affects thoracic injury outcomes across a wide range of pedestrian scenarios. Additionally, [14] specifically demonstrated that in sedan-type vehicle impacts, allowing or restricting upper extremity contact with the vehicle has a considerable influence on thoracic injury severity.

In total, 240 HBM simulations were executed, 48 per vehicle variant, using VPS version 2023. Each simulation was targeted to run for 200 milliseconds, with the vehicle impacting the HBM from the left side at 40 km/h. A friction coefficient of 0.3 was applied between the vehicle and the HBM, consistent with Euro NCAP TB024 guidelines.

To ensure the HBM simulations were suitable for analysis, each simulation was reviewed to confirm that it either terminated normally or progressed beyond the point of maximum thorax contact force before encountering an error termination. Only simulations in which the HBM thorax interacted with areas of the vehicle covered by the headform impactor test area were considered for further evaluation.

For each simulation, the maximum probabilities of AIS2+ and AIS3+ thoracic (rib cage) injuries were calculated using the developed injury risk functions. Simulations with injury probabilities exceeding 50% were flagged for further attention. The time corresponding to the peak thorax contact force, referred to as the Time of maximum thorax ContacT force (TCT), was recorded, as this moment was assumed to represent the highest likelihood of injury.

At TCT, a simulation frame was extracted for each qualifying case to visually document the interaction between the vehicle and the HBM's thorax (skeletal ribcage). Within this frame, the rib area was precisely delineated (see Fig. 5), and all HIC15 values from the headform impactor target points falling within this marked region were identified. The maximum HIC15 value among values within the marked frame was then recorded for further analysis.

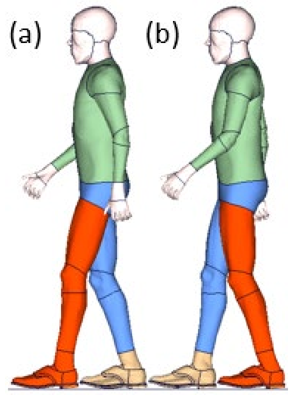

Fig. 2. Leg Positions: (a) LLF, (b) LLB

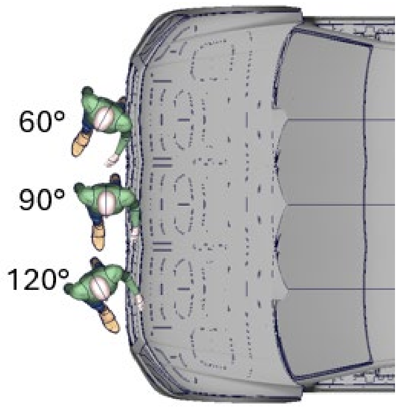

Fig. 3. HBM Orientation

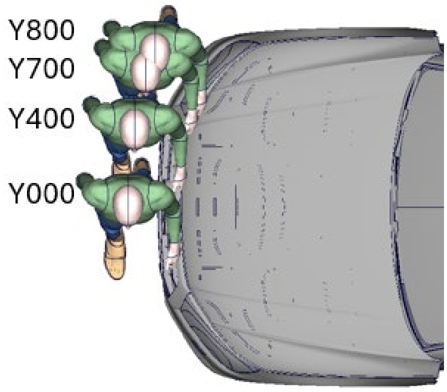

Fig. 4. HBM Position along Y-axes

The final analysis focused on identifying simulations that met two key criteria:

1. A thoracic injury probability greater than 50%, and
2. HIC15 values were evaluated against defined threshold of 650 (±50) to determine whether they fell above or below these thresholds.

The 650 threshold is particularly important, as it represents the Euro NCAP's upper limit for achieving maximum scoring. A ±50 range around this benchmark was included to evaluate the sensitivity of the relationship between HIC values and thoracic injury risk.

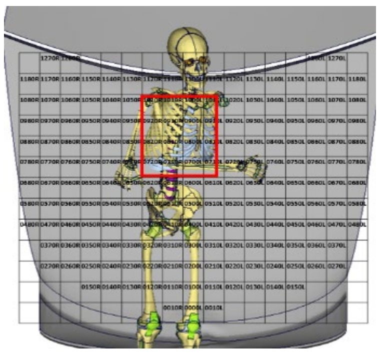
Fig. 5. Marking of the Ribcage

III. RESULTS

Table 1 summarizes the usability of the HBM simulations for further analysis, indicating that five simulations encountered error termination. Among these five, three cases were deemed *Usable* since the TCT occurred before the simulation terminated. The remaining two were deemed *Unusable*, either due to thorax non-contact till the termination time or because the TCT occurred at the point of error termination. However, it should be noted that the termination of any simulations was not related to the HBM. Consequently, a total of 238 simulations were deemed *Valid*. During the analysis, it was observed that in most simulations with an initial Y-location at Y800, and in some cases at Y700, the HBM thorax made little or no contact with the vehicle bonnet region (Fig. 6) evaluated by the headform impactor. These cases were marked as "*No-CNT*" in Table II.

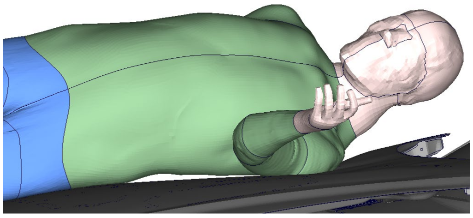

Fig. 6. No contact between thorax and vehicle

Table I
SIMULATION CLASSIFICATION

Vehicle Model Variant	Termination			Valid	DSC	Qualified	Total
	Normal	Error					
		U	UN				
SUV-1-P	47	1	0	48	12	35	48
SUV-1-D	48	0	0	48	12	36	48
Sedan-P	46	2	0	48	12	36	48
Sedan-D	46	0	2	46	13	33	48
SUV-2-P	48	0	0	48	13	35	48
Total	235	3	2	238	63	175	240

P – Passive Bonnet, D – Deployed Bonnet, U – Usable, UN – Unusable, DSC – Discarded

TABLE II
SUMMARY OF DISCARDED CASES

Vehicle	SUV1		Sedan		SUV2	
Configuration	WCNT	WoCNT	WCNT	WoCNT	WCNT	WoCNT
D_EuLLB_060_400	Q	Q	UN	Q	-	-
D_EuLLB_060_800	LT	LT	No - CNT	No - CNT	-	-
D_EuLLB_090_700	Q	Q	No - CNT	Q	-	-
D_EuLLB_090_800	LT	LT	No - CNT	No - CNT	-	-
D_EuLLB_120_800	LT	LT	No - CNT	LT	-	-
D_EuLLF_060_800	LT	LT	GT	GT	-	-
D_EuLLF_090_800	LT	LT	LT	LT	-	-
D_EuLLF_120_400	Q	Q	UN	Q	-	-
D_EuLLF_120_800	LT	GT	LT	LT	-	-
P_EuLLB_060_700	No - CNT	Q	Q	Q	Q	Q
P_EuLLB_060_800	No - CNT	No - CNT	No - CNT	No - CNT	No - CNT	LT
P_EuLLB_090_800	LT	LT	No - CNT	No - CNT	LT	LT
P_EuLLB_120_700	Q	Q	Q	Q	LT	Q
P_EuLLB_120_800	LT	LT	LT	LT	No - CNT	LT
P_EuLLF_060_800	LT	LT	GT	GT	LT	LT
P_EuLLF_090_800	LT	LT	LT	LT	LT	LT
P_EuLLF_120_800	LT	LT	LT	LT	LT	LT

Q – Qualified (included for further analysis), LT – Less than threshold, Greater than threshold, CNT – Contact
Configuration: (<Bonnet>_<Posture>_<HBM-Orientation>_<Y-Location>)
Bonnet: Deployed (D) / Passive (P)

In many simulations at positions Y700 and Y800, the HBM thorax made contact with the vehicle; however, the interaction was often minimal, as indicated by very low thorax contact forces. To systematically classify these cases, a thorax contact force threshold was applied. A value of 1200 N was selected based on findings from previous studies on frontal [32], as well as lateral and oblique [33] thoracic impacts, which reported the forces around 1200 N level as non-injurious. Simulations with thorax contact forces below 1200 N were labeled as "*LT*" (Lower than Threshold), while those with forces equal to or exceeding 1200 N were labeled as "*GT*" (Greater than Threshold), as shown in Table II.

Each *LT* and *GT* was further examined to determine whether thorax contact occurred within the area assessed by the headform impactor. Notably, in all *GT* cases, the thorax contacted regions that were either entirely outside the headform impactor test area or limited to very small areas within zones associated with elevated HIC values. Representative examples of these interactions are provided in Fig. A3. Including *LT* cases would compromise the interpretation of results, as they combine low thoracic injury probability with disproportionately high HIC values. Whereas *GT* cases, impacts occurred outside or only minimally within the areas evaluated with headform tests, were not suitable for hypothesis check. To avoid skewing the analysis, 63 of the 238 valid simulations were excluded from further analysis. These cases are marked as "*Discarded*" in Table I.

Following this filtering process, 175 simulations were retained for detailed analysis. This set included 172 simulations that completed normally and three additional cases that, despite early termination, provided usable data. All retained simulations are referred to as "*Qualified*" in Table I. It is important to note that qualification outcomes varied across impact configurations, as differences in post-impact kinematics led some cases to meet the inclusion criteria while others were excluded. Although Table II is intended to summarize only the *Discarded* cases, some configurations included both *Qualified* and *Discarded* outcomes. For clarity, the qualified cases are also marked as '*Q*' within the table.

Table III summarizes the key findings from the 175 qualified simulations. Injury/No-Injury information for each case is provided in Table A1 in Appendix 1 for the reference. Among qualified cases, 43 simulations exhibited a thoracic injury probability (AIS2+) exceeding 50%, while only seven simulations exceeded 50% threshold for AIS3+ injury probability. Given that AIS3+ injuries occurred in fewer than 3% of the 238 valid simulations, the subsequent analysis focused exclusively on AIS2+ outcomes.

TABLE III
HYPOTHESES CHECK FOR THORACI INJURY

Vehicle Variant	AIS3+ Cases	AIS2+ Cases	HIC 600		HIC650		HIC700	
			HIC>600, AIS2>50%	HIC<600, AIS2>50%	HIC>650, AIS2>50%	HIC<650, AIS2>50%	HIC>700, AIS2>50%	HIC<700, AIS2>50%
SUV1-P	1	9	9	0	9	0	9	0
SUV1-D	1	10	10	0	10	0	10	0
Sedan-P	5	14	14	0	14	0	14	0
Sedan-D	0	8	7	1	6	2	6	2
SUV2-P	0	2	2	0	2	0	2	0
Total	7	43	42	1	41	2	41	2

The sedan accounted for the highest number of AIS2+ injuries (22 cases), despite having fewer qualified simulations (71) compared to the combined total of 104 simulations for the two SUV models. A notable trend emerged regarding bonnet type: simulations involving a deployed bonnet resulted in significantly fewer AIS2+ injuries compared to those with a passive bonnet.

When examining the influence of upper extremity contact, simulations with contact (WCNT) showed 11 AIS2+ injuries for SUV1, one for SUV2, and eight for the sedan. In contrast, simulations without contact (WoCNT) showed eight AIS2+ injuries for SUV1, 13 for the sedan, and one for SUV2.

Pedestrian posture also played a vital role in injury outcomes. Simulations with the EuLLB posture resulted in 18 AIS2+ injuries, while those with the EuLLF posture resulted in 25. In all simulations, the left side was the impacting side. Regarding pedestrian orientation, the 90° orientation led to the highest number of injuries (19 cases), followed by 120° (13 cases) and 60° (11 cases).

A further analysis was conducted to check if thoracic AIS2+ injury probability exceed 50% even when the corresponding HIC15 values from headform tests remained below the selected threshold of 650 (±50). As it can be noted from Table III, among the 175 qualified simulations, such exceptions were identified in one case for the 600 threshold, and two cases each for the 650 and 700 thresholds. All of these exceptions involved the sedan with a deployed bonnet and are labeled as "*Sedan-D-Fail*" in subsequent discussions. In each of *Sedan-D-Fail* cases, upper extremity contact was deactivated. The initial Y-locations were either Y000 (with a 120° orientation) or Y400 (with a 90° orientation), and the pedestrian postures were LLF for Y000 and LLB for Y400.

IV. DISCUSSION

Based on the insights from the accident databases, regulatory protocols and safety assessment, guidelines have been developed to evaluate the performance of vehicle front structures (shape as well as stiffnesses) that commonly poses risk to the pedestrian head and lower extremities. Consequently, over the past few decades, considerable efforts have been directed toward preventing and mitigating head and lower extremity injuries in vehicle–pedestrian collisions. Typically, bonnet stiffness and the clearance between the bonnet and underlying hard structures are optimized to reduce the severity of head injuries, in line with regulatory requirements and consumer safety rating protocols. However, as recent studies have sought more insight into thoracic injury risk, an important question arises: do bonnet designs optimized to meet legislative and consumer rating requirements for pedestrian head injury mitigation also offer adequate protection to the thorax, or is there a need for additional design considerations to address thoracic injury risk?

In the present study, across 238 valid simulations, AIS3+ thoracic injuries were noted in less than 3% cases. This low incidence is likely due to vehicle designs that comply with pedestrian protection regulations, particularly through optimized bonnet stiffness and structural clearance. Such a low number of AIS3+ injuries would not help for a meaningful evaluation of the hypothesis. Hence, the study focused on AIS2+ (observed in around 18% cases) thoracic injury probability.

From the simulations that terminated abnormally, where the peak thorax contact force occurred at the error termination time, were excluded, as continued simulation might have resulted in different outcomes. Additionally, all simulations at Y800 and selected cases at Y700 were excluded due to minimal or absent thoracic contact in the areas tested by headform impactors, despite high HIC values caused by stiffer lateral structures. Including such cases would have skewed the dataset toward high HIC but low thoracic injury probability, distorting the interpretation. Simulations with no measurable thorax-to-bonnet contact force were also excluded.

For most of the qualified 175 cases, the AIS2+ thoracic injury probability remained under 50% threshold where HIC values were 650 or less. Notably, two *Sedan-D-Fail* cases were identified, where the AIS2+ thoracic injury probability exceeded 50%, but the HIC values remained below 650. Both occurred in simulations involving a deployed bonnet and zones with a relatively large clearance between the bonnet and the underlying structure. As it can be observed in Fig. 7, following shoulder impact, the bonnet deformed locally, which partially limited further motion of the shoulder. While the shoulder's movement was restricted, the rest of the HBM continued to move due to inertia, generating shear forces at the vehicle-shoulder interface. As it can be observed in the sequence with skeleton, the impacting side ribs were subjected not only to direct lateral compression but also to bending due to inferior-superior reaction at the shoulder.

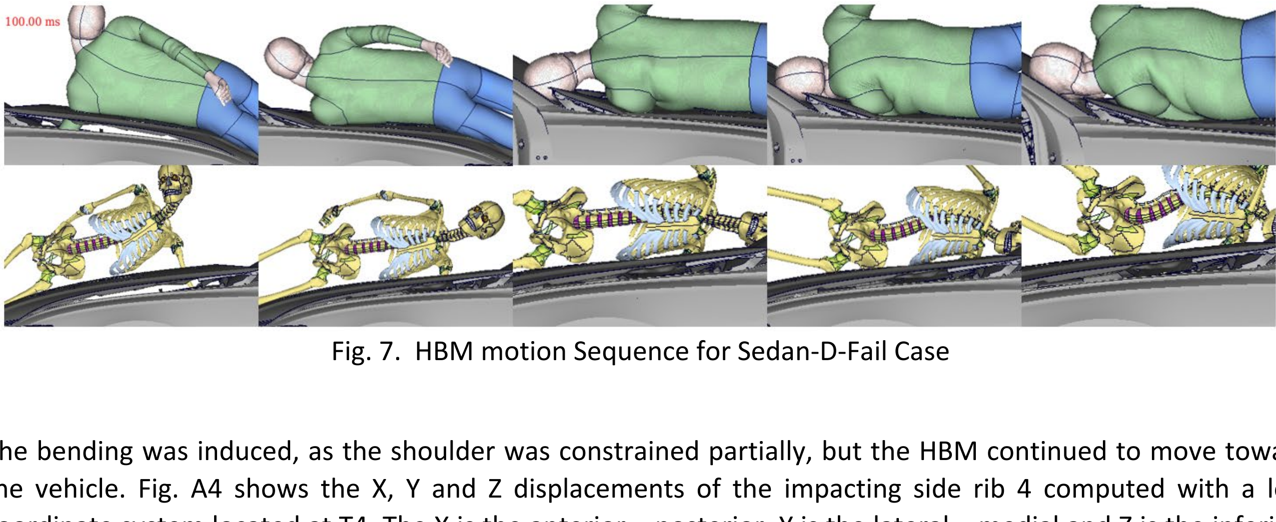

Fig. 7. HBM motion Sequence for Sedan-D-Fail Case

The bending was induced, as the shoulder was constrained partially, but the HBM continued to move towards the vehicle. Fig. A4 shows the X, Y and Z displacements of the impacting side rib 4 computed with a local coordinate system located at T4. The X is the anterior – posterior, Y is the lateral – medial and Z is the inferior –

superior direction. As can be noted from the Fig. A4, the value of inferior – superior displacement of the rib is considerably high. Authors believe that the deformation due to the combination of the lateral compression and out of plane bending must have led to the increased risk of AIS2+ injuries. The cases like *Sedan-D-Fail* demonstrate the complexities of the injury mechanism to the pedestrian thorax. Although similar combined loading was observed in other simulations, the resulting rib deformations were less severe than in the *Sedan-D-Fail* cases.

A few studies in recent years have explored various approaches to evaluating thoracic injuries in vehicle–pedestrian collisions. For instance, [15] introduced the Thorax Injury Prediction Tool (TIPT) as a method for assessing thoracic injury risk. However, the TIPT has certain limitations. It is based on the EUROSID2 dummy torso, which lacks the capability to capture rib deformations such as bending—an important injury mechanism observed in cases like *Sedan-D-Fail*. Another study explored the correlation between headform impactor acceleration and ribcage deflection using simulations at the Y000 location [20]. However, the limited number of scenarios used in the study [20] did not represent the full range of vehicle regions likely to interact with the thorax.

A more comprehensive approach was taken in [19], which included four Y-locations and a headform impactor test grid to examine the correlation between HIC values and rib deformation. However, [19] did not account for variations in vehicle type, bonnet configuration (active vs. passive), or pedestrian posture and orientation, all of which, as observed in the present study, exert a considerable influence on the thoracic injury outcomes

In contrast, the present study employs a more robust and comprehensive simulation matrix, encompassing a broader range of vehicle categories, bonnet configurations, pedestrian postures, orientations, and lateral impact locations. This expanded scope enabled a more nuanced evaluation of the hypothesis that bonnets optimized for head injury mitigation may also enhance thoracic safety.

In the present study, Sedan is found to associated with higher number of thoracic injuries compared to SUVs. These findings are consistent with the previous studies [14], and observations of [16] who reported higher thoracic impact velocity in case of sedan relative to other vehicle types.

Additionally, the interaction between the upper extremities and the vehicle structure was found to influence injury outcomes. However, the effect varied case to case. For instance, under WCNT (with contact) conditions, the number of AIS2+ thoracic injuries increased in SUVs but decreased in sedans. This suggests that the role of upper interaction is context dependent.

Pedestrian posture also played a significant role. AIS2+ thoracic injuries occurred more frequently when the impacting-side leg was in the forward position (EuLLF) compared to the backward position (EuLLB). These variations indicate that detailed, case-by-case investigations are necessary to better understand the parameters contributing to injury frequency.

Despite these variations, and aside from two outlier cases such as *Sedan-D-Fail*, thoracic injuries were consistently lower in regions where HIC values remained below the regulatory threshold. This suggests that vehicle designs optimized to meet current pedestrian head protection standards may also offer adequate protection for the thorax, potentially reducing the need for additional thorax-specific testing.

While the study offers a comprehensive simulation matrix to address various attributes related to vehicle – pedestrian impacts, few limitations should be acknowledged. For instance, only one pedestrian size and gender (50^{th} percentile male) was considered. Secondly, simulations were limited to two postures and a specific set of orientations. Moreover, muscle activation effects were not modelled. Due to the limitations of the modelling, only osteal thorax injuries were analysed, excluding other thoracic structures (e.g., internal organs). However, given the limitations of the modelling and data, most of the studies uses the rib cage injuries as a representative of the thoracic injuries. The study demonstrates that headform impact zones with low HIC values generally correspond to low thoracic injury probabilities, but it does not establish a causal relationship i.e., that reducing HIC directly results in reduced thoracic injury. To prove such a causal link, a dedicated sensitivity study would be required, involving controlled modifications to bonnet stiffness and structure while holding other parameters constant. Also, the findings may not be generalised to larger vehicles, such as pickups or large SUVs typical in the United States, where pedestrian thorax often contacts with the vehicle front parts other than the bonnet.

V. CONCLUSION

This study employed FE simulations using a validated HBM and production vehicle models to investigate thoracic injury risks in pedestrian–vehicle collisions. A range of pedestrian, vehicle, and event-related parameters were considered to capture the complexity of real-world crash scenarios. Across 238 valid simulations, AIS3+ thoracic injuries (with estimated probability more than 50%) were observed in less than 3% of cases, while AIS2+ injuries (estimated probability more than 50%) occurred in around 18% of the valid cases. Notably, in all but two simulations, the probability of sustaining an AIS2+ thoracic injury remained below 50% when the HIC value computed from the headform impactor simulation was under 650; the two exceptions, identified as outliers, were attributed to the complex nature of the loading conditions.

The mechanisms and severity of thoracic injuries were found to be complex, influenced by factors such as vehicle type and bonnet deployment, as well as the posture, orientation, and impact location of the pedestrian. Nevertheless, the analysis indicates that the current headform impactor protocols, as outlined in existing consumer safety guidelines, effectively reflect the level of thoracic injury protection provided by the assessed bonnet areas and additional thoracic-specific assessments may be redundant for the vehicle fleets considered in this study.

VI. ACKNOWLEDGEMENTS

The authors would like to thank AUDI AG and Volkswagen AG for supporting this study. Authors also thank Mr. Stefan Schinke and Mr. Olaf Insel from Volkswagen AG for their insightful suggestions during the project and reviewing the manuscript.

VII. REFERENCES

[1] Hu, J. (2023) NHTSA, Pedestrian Safety: Assessment of Crashworthiness Test Procedures, USA.

[2] World Health Organization, Global status report on road safety 2023, Geneva. (Accessed March 13, 2025)

[3] Saadé, J., Cuny, S., Labrousse, M., Song, E., Chauvel, C., Chrétien, P., (2020) Pedestrian Injuries and Vehicles-related Risk Factors in Car-to-pedestrian Frontal Collisions. *Proceedings of IRCOBI 2020 Conference, Munich, Germany.* (Online).

[4] Anderson, R., McLean, J., Streeter, L., Ponte, G., Sommariva, M., Lindsay, T. and Wundersitz, L., (2002) Severity and Type of Pedestrian Injuries Related to Vehicle Impact Locations and Results of Sub-System Impact Reconstruction. *Proceedings of IRCOBI 2002 Conference, Munich, Germany.*

[5] Cookson, R., Cuerden, R., Richards, D., Rutter, H., (2009), Pedestrian injury characteristics following road traffic collisions. *Proceedings of 21st ESV Conference*, Stuttgart, Germany.

[6] Martin, J.-L., Lardy, A., Laumon, B., (2011), Pedestrian Injury Patterns According to Car and Casualty Characteristics in France. *Proceedings of 55th AAAM Annual Conference*, Paris, France.

[7] Värnild, A., Tillgren, P., Larm, P., (2020) What types of injuries did seriously injured pedestrians and cyclists receive in a Swedish urban region in the time period 2003 – 2017 when Vision Zero was implemented?. Public Health, 181: 59 – 64.

[8] Schneider, A., Ewald, C., Roth, F., Labenski, V., Sherwood, C., Crandall, JR. (2019) Development of a combined Injury Criteria for the comparative Evaluation of Long-term Injury Outcome and Mortality Risk assessed in Car-to-Pedestrian Accidents. *Proceedings of IRCOBI 2019 Conference, Florence, Italy.*

[9] Staack, H., Labenski, V. (2022), Thorax Injuries in VRU Accidents – an Evidence-based Approach. *Proceedings of IRCOBI 2022 Conference, Porto, Portugal.*

[10] Staack, H., Labenski, V., Marini, G., Liang, Y., (2023), Comparison of Chinese and German in-depth accident data of pedestrian thorax and head injuries, *Proceedings of 67th Stapp Car Crash Conference, 2023*, Michigan, USA.

[11] Koizumi, Y. (2024), A study on pedestrian thoracic injuries in Chinese market based on CIDAS data. CIDAS annual meeting 2024, People's Republic of China

[12] Zegeer, CV, Bushell, M., (2012). Pedestrian crash trends and potential countermeasures from around the world."Accid Anal Prev 44(1): 3-11.

[13] European Commission - Road safety thematic report – Pedestrians (2020-2023 data) (2023); European Road Safety Observatory. Brussels, European Commission, Directorate General for Transport.

[14] Jani, D., Lehmann, K., Staack, H., Teichmann, C., Marini, G. (2023) Numerical investigations on the factors affecting thorax injuries in vehicle vs pedestrian accidents. *Proceedings of 67th Stapp Car Crash Conference, 2023*, Michigan, USA.

[15] Zander, O., Wisch, M., Ott, J., Burleigh, M., Fornells, A., Lundgren, C. (2019) Development and evaluation of a Thorax Injury Prediction Tool (TIPT) and possibilities for incorporation within improved test and assessment procedures – results from SENIORS. *Proceedings of 26th ESV Conference*, Eindhoven, Netherlands.

[16] Pal, C., Hirayama, S., Vallabhaneni, P.N., Kulothungan, V. (2023) Influence of Different Parameters of Vehicle and Pedestrian on Chest Kinematics Using Human Body Model (HBM). *m 27th ESV Conference*, Yokohama, Japan.

[17] Watanabe, R., Katsuhara, T., Miyazaki, H., Kitagawa, Y., Yasuki, T. (2012) Research of the Relationship of Pedestrian Injury to Collision Speed, Car-type, Impact Location and Pedestrian Sizes using Human FE model (THUMS Version 4). Stapp Car Crash Journal 56: 269-321.

[18] Chen, H., Poulard, D., Crandall, J.R., Panzer, M.B. (2015) Pedestrian response with different initial positions during impact with a mid-sized sedan. *Proceedings of 24th ESV Conference*, Gothenburg, Sweden.

[19] Sogabe, H. (2023), A study on the relationship between pedestrian thorax injury and head injury criterion at passenger car to pedestrian collision; CIDAS Annual Meeting 2023, People's Republic of China

[20] Han, Y., Yang, J., Mizuno, K., Matsui, Y. (2012), A study on chest injury mechanism and the effectiveness of a headform impact test for pedestrian chest protection from vehicle collisions. Safety Science. 50 (1304-1312).

[21] Euro NCAP (2023), European New Car Assessment Programme – Vulnerable Road User Testing Protocol v9.1 (dated December 5, 2023)

[22] https://de.statista.com/statistik/daten/studie/316701/umfrage/pkw-neuzulassungen-in-deutschland-segmente/

[23] https://www.umweltbundesamt.de/daten/verkehr

[24] UN Regulation No. 127 Revision 2 (2016) Uniform provisions concerning the approval of motor vehicles with regard to their pedestrian safety performance.

[25] Teichmann, C. (2020) A comparison between aPLI and HBM simulation, 15th Praxis Conference Pedestrian Protection, Bergisch Gladbach, Germany.

[26] Vieler, C., Marini, G., Sahoo, D., Wagner, K., Neumann, F., Glass, E., Schuller, A. (2024) Overview of Advancement and Application of HBMs in VW Group, Human Modeling and Simulation in Automotive Engineering Symposium, Marburg, Germany.

[27] Sahoo, D., Jani, D., Marini, G., (2024) Validation THUMSv4.1 head model in Visual Performance Solution and development of model-specific head injury criteria: skull fracture, mild Diffuse Axonal injury and subdural haematoma, *Proceedings of IRCOBI 2024 Conference*, Stockholm, Sweden.

[28] Forman, J., Joodaki, H., Forghani, A., Riley, P., Bollapragada, V., Lessley, D., Overby, D., Heltzel, S., Crandall, J. (2015), Biofidelity Corridors for Whole-Body Pedestrian Impact with a Generic Buck. *Proceedings of IRCOBI 2015 Conference*, Lyon, France.

[29] Song, E., Petit, P., Trosseille, X., Uriot, J., Pascal, P., Dubois, D., Douard, R. (2017) New Reference PMHS Tests to Assess Whole-Body Pedestrian Impact Using a Simplified Generic Vehicle Front-End. Stapp Car Crash Journal 61: 299-354.

[30] Klug, C., Ellway, J., (2023) Technical Bulletin TB024 – Pedestrian Human Model Certification Version 4.0 (dated July 2023).

[31] Forman, J., Kulkarni, S., Perez-Rapela, D., Mukherjee, S., Panzer, M., Hallman, J. (2022) A Method for Thoracic Injury Risk Function Development for Human Body Models. *Proceedings of IRCOBI 2022 Conference*, Porto, Portugal.

[32] Murach, M.M., Kang, Y-S, Bolte IV J.H., Stark, D., Ramachandran, R., Agnuew, A., Moorhouse, K., Stammen, J. (2018) Quantification of Skeletal and Soft Tissue Contributions to Thoracic Response in a Dynamic Frontal Loading Scenario, Stapp Car Crash Journal, 62: 193-269.

[33] Shaw, J.M., Herriott, R.G., McFadden, J.D., Donnelly, B.R., Bolte IV J.H. (2006) Oblique and Lateral Impact Response of the PMHS Thorax, Stapp Car Crash Journal, 50: 147-167.

VIII. APPENDIX

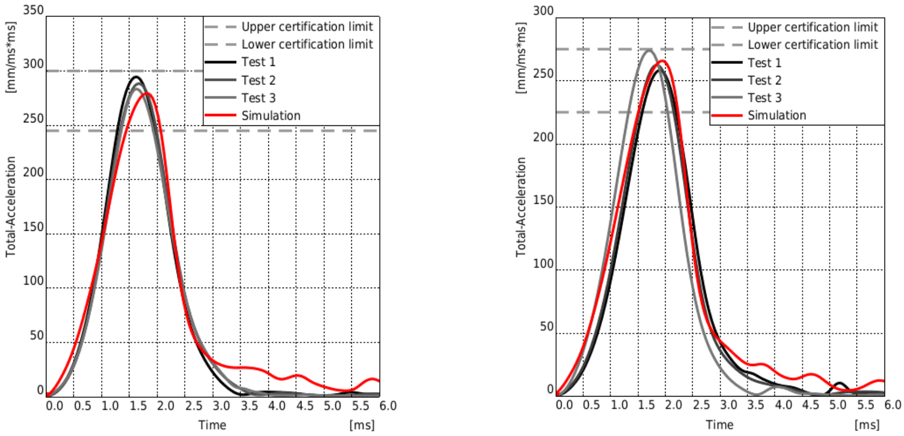

Fig. A1 Child (Left) and Adult(Right) headform impactors validation

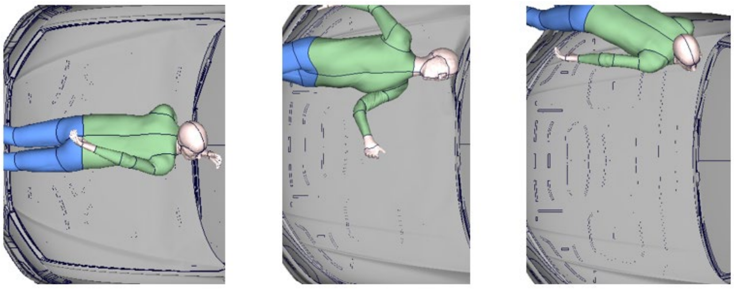

Fig. A2 Position of HBM thorax on the vehicle front

Configuration: WO_SUV1_P_EuLLF
Contact: Near A-Pillar, Outside Test Area

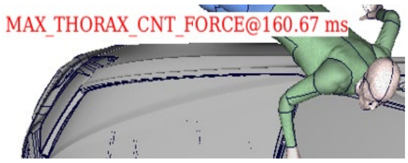

Configuration: W_SEDAN_P_EuLLF
Contact: Near A-Pillar, Outside Test Area

Configuration: W_SUV2_P_EuLLF
Contact: Near A-Pillar, Outside Test Area

W: WCNT
WO: WoCNT
P: Passive Bonnet

Fig. A3 HBM Position in Selected Discarded Cases at Maximum Thorax Contact Force

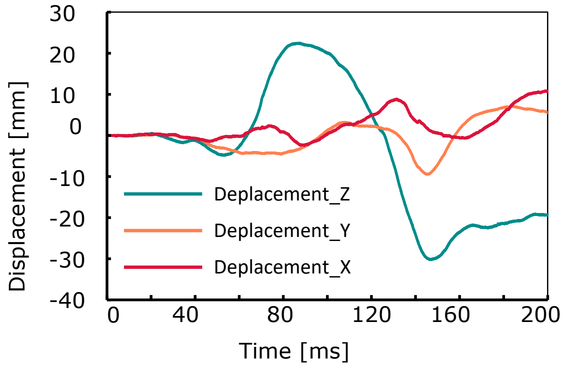

Fig. A4 Displacements of node of the impacting side rib 4 along X, Y and Z directions for the Sedan – D – Fail case. Z is the inferior – superior direction of the local coordinate system at T4.

TABLE A1
AIS2+ THORACIC INJURY LIKELYHOOD FOR QUALIFIED CASES

Vehicle	**SUV1**		**Sedan**		**SUV2**	
Configuration	**WCNT**	**WoCNT**	**WCNT**	**WoCNT**	**WCNT**	**WoCNT**
D_EuLLB_060_000L	I	I	NI	NI	-	-
D_EuLLB_060_400R	I	NI	UN	NI	-	-
D_EuLLB_060_700R	NI	NI	NI	NI	-	-
D_EuLLB_090_000L	I	I	NI	NI	-	-
D_EuLLB_090_400R	NI	NI	NI	I	-	-
D_EuLLB_090_700R	NI	NI	NI	NI	-	-
D_EuLLB_120_000L	NI	NI	NI	NI	-	-
D_EuLLB_120_400R	NI	NI	NI	NI	-	-
D_EuLLB_120_700R	I	NI	NI	I	-	-
D_EuLLF_060_000L	NI	I	NI	NI	-	-
D_EuLLF_060_400R	NI	NI	NI	NI	-	-
D_EuLLF_060_700R	NI	NI	NI	I	-	-
D_EuLLF_090_000L	I	I	NI	NI	-	-
D_EuLLF_090_400R	I	NI	I	NI	-	-
D_EuLLF_090_700R	NI	NI	NI	NI	-	-
D_EuLLF_120_000L	NI	NI	I	I	-	-
D_EuLLF_120_400R	NI	NI	UN	NI	-	-
D_EuLLF_120_700R	NI	NI	I	I	-	-
P_EuLLB_060_000L	I	I	NI	NI	NI	NI
P_EuLLB_060_400R	NI	NI	NI	NI	NI	NI
P_EuLLB_060_700R	NI	NI	NI	I	NI	NI
P_EuLLB_090_000L	I	I	NI	NI	NI	NI
P_EuLLB_090_400R	NI	I	NI	I	NI	I
P_EuLLB_090_700R	NI	NI	NI	I	NI	NI
P_EuLLB_120_000L	NI	NI	NI	NI	NI	NI
P_EuLLB_120_400R	NI	NI	NI	NI	NI	NI
P_EuLLB_120_700R	NI	NI	NI	I	DISC	NI
P_EuLLF_060_000L	NI	I	NI	NI	NI	NI
P_EuLLF_060_400R	NI	NI	NI	NI	NI	NI
P_EuLLF_060_700R	NI	NI	I	I	NI	NI
P_EuLLF_090_000L	I	NI	I	NI	NI	NI
P_EuLLF_090_400R	I	NI	I	NI	I	NI
P_EuLLF_090_700R	I	NI	NI	NI	NI	NI

P_EuLLF_120_000L	NI	NI	I	I	NI	NI
P_EuLLF_120_400R	NI	NI	I	I	NI	NI
P_EuLLF_120_700R	NI	NI	I	I	NI	NI

Configuration: <Bonnet>_<Posture>_<HBM-Orientation>_<Y-Location>
Bonnet: Deployed (D) / Passive (P)
I: Injury
NI: No – Injury
DISC: Discarded
UN: Unusable